ORIGINAL PAPER

One Pot Synthesis, Photophysical and X-ray Studies of Novel Highly Fluorescent Isoquinoline Derivatives with Higher Antibacterial Efficacy Based on the In-vitro and Density Functional Theory

Abdullah M. Asiri · Salman A. Khan ·
Saad H. Al-Thaqafy · Kamlesh Sharma

Abstract Series of cyano substituted isoquinoline dyes were synthesized by one-pot multicomponent reactions (MCRs) of aldehydes, malononitrile, 6-methoxy-1,2,3,4-tetrahydro-naphthalin-1-one and ammonium acetate. Results obtained from spectroscopic (FT-IR, ^{1}H-NMR, ^{13}C-NMR, EI-MS) and elemental analysis of synthesized compounds was in agreement with their chemical structures. Structure of the compound was further conformed by X-ray crystallographic. UV-vis and fluorescence spectroscopy measurements provided that all compounds are good absorbent and fluorescent. Fluorescence polarity study demonstrated that these compounds were sensitive to the polarity of the microenvironment provided by different solvents. In addition, spectroscopic and physicochemical parameters, including electronic absorption, extention coefficient, Stokes shift, oscillator strength transition dipole moment and fluorescence quantum yield were investigated in order to explore the analytical potential of synthesized compounds. The anti-bacterial activity of these compounds were first studied in vitro by the disk diffusion assay against two Gram-positive and two Gram-negative bacteria. The minimum inhibitory concentration was then determined with the reference of standard drug chloramphenicol. The results displayed that compound **3** was better inhibitors of both types of the bacteria (Gram-positive and Gram-negative) than chloramphenicol. Furthermore, quantum chemistry calculations using DFT/6-31-G* level of theory confirm the results. Dipole moment and frontier molecular orbitals were also investigated.

Keywords Isoquinoline · Dipole moment · Anti-bacterial activity · Chloramphenicol · Quantum chemistry

A. M. Asiri · S. A. Khan (✉) · S. H. Al-Thaqafy
Chemistry Department, Faculty of Science, King Abdulaziz University, Jeddah 21589, P.O. Box 80203, Saudi Arabia
e-mail: sahmad_phd@yahoo.co.in

A. M. Asiri
Center of Excellence for Advanced Materials Research (CEAMR), King Abdulaziz University, Jeddah 21589, P.O. Box 80203, Saudi Arabia

K. Sharma
Department of Applied Science, School of Engineering & Technology, ITM University, Sector 23A, Gurgaon 122017, India

Introduction

Nitrogen containing heterocyclic compounds such as pyrazoline, pyrazole qnoxaline quinoline, pyrimidene are compounds that have been studied for a considerable period of time for their biological properties [1]. Quinoline derivatives are one of the most applicable compounds in the filed of the medical chemistry [2]. Its traces of interest date back to the beginning of the 20th century but the first reports on their medical applications began to appear in the Fifties as antibiotic drugs against tuberculosis and leprosy [3]. Quinoline derivatives are of considerable interest because of their chemistry and potentially beneficial biological activity, such as antibacterial, antifungal, antiviral, antiamoebic, antimalarial and antitumor activity [4–7]. Quinoline derivatives use as intermediate for the formation of various fused bi-cyclic heterocyclic compounds such as pyrazolo quinoline, thiazolo quinoline, oxazolquinoline [8–10]. Cyano substituted 2-amino isoquinoline are use as ligands in the field of inorganic chemistry for the formation of metal complexes with Cu(II), Ni(II), Co(II), Pt (II), Pd(II), Cd(II) and (Zn (II)due to presence of

nitrogen and amine group [11]. Several reactions were reported for the synthesis of quinoline derivatives through ring annulations, intermolecular and intramolecular cyclization [12]. All these type reaction are multi steps reaction and low harsh reaction conditions and relatively overall low yields [13]. On the other hand, pyridine derivatives are widely used in materials science fields, such as, third order non-linear optics (NLO) [14], optical switching [15], electrochemical sensing [16], langmuir films and photoinitiated polymerization [17]. Physicochemical characteristics, such as, solvatochromic, piezochromic, oscillator strength, dipole moment, fluorescent quantum yield and photostability, are also most important studies for determining the behavior of compounds [18]. People are working from last many years on the synthesis and characterization of quinoline by multi set reaction with their biological application but very little work has been done so far on cyano substituted isoquinoline. 2-Amino cyano substituted isoquinoline are promising as new class of experimental anti-cancer chemotherapeutic agents which shows evidence of inhibitory behavior against cancer [19]. These are also a useful model for bioinorganic processes [20, 21]. Due to wide range of application of the cyano substituted isoquinoline, we have synthesized, novel 2-amino cyano substituted isoquinoline and their antibacterial activity on the bases of in-vitro, and density functional theory and their physicochemical studies such as electronic absorption, molar absorptivity, oscillator strength, dipole moment and fluorescence quantum yield are also determine.

Experimental

Chemicals and Reagents

The appropriate aldehyde, 6-methoxy-1,2,3,4-tetrahydronaphthalin-1-one, malononitrile and ammonium acetate were purchased from Acros Organic. Other reagents and solvents (A.R.) were obtained commercially and used without further purification, except dimethylformamide (DMF), ethanol and methanol.

Apparatus

Melting points were recorded on a Thomas Hoover capillary melting apparatus without correction. FT-IR spectra were recorded on a Nicolet Magna 520 FT-IR spectrometer. ^{1}H-NMR and ^{13}C-NMR experiments were performed in CDCl$_3$ on a Brucker DPX 600 MHz spectrometer using tetramethyl silane (TMS) as internal standard at room temperature. UV-vis electronic absorption spectra were acquired on a Shimadzu UV-1650 PC spectrophotometer. Absorption spectra were collected using a 1 cm quartz cell. Steady state fluorescence spectra were measured using Shimadzu RF 5301 PC spectrofluorphotometer with a rectangular quartz cell. Emission spectra were monitored at right angle. All fluorescence spectra were blank subtracted before proceeding in data analyses.

General Method for the Synthesis of Benzoquinoline Derivatives (1–5)

A one-pot mixture of the appropriate aldehyde (0.011 mol), 6-methoxy-1,2,3,4-tetrahydro-naphthalin-1-one (2 g, 0.011 mol), malononitrile (0.74 g, 0.011 mol) and ammonium acetate (6.78 g, 0.088 mol) in absolute ethanol (25 mL) was refluxed for 6 h [22]. The reaction mixture was allowed to cool, and the resulting precipitate was filtered, washed with water, dried and recrystallized from ethanol and chloroform.

2-amino-4-[4-(dimethylamino)phenyl]-9-methoxy-5,6 dihydrobenzo[f]isoquinoline-1-carbonitrile (1)

EI-MS m/z (rel. int. %): 372 (72) [M+1]$^{+}$; IR (KBr) v_{max} cm^{-1}: 3412 (NH$_2$), 2980 (C-H), 2218 (CN), 1575 (C=C); ^{1}H NMR (600MXz CDCl$_3$) δ: 8.23 (d, 1H, CH$_{Ar}$, J= 8.4 Hz), 7.85 (d, 1H, CH$_{Ar}$, J=8.4 Hz), 7.26 (d,1H, CH$_{Ar}$), 7.50 (s, 1H, CH$_{Ar}$), 6.75 (d, 1H, CH$_{Ar}$, J=2.4 Hz), 6.90 (d, 1H, CH$_{Ar}$, J=2.4 Hz), 5.10 (s,2H, NH$_2$), 3.88 (s, 3H, OCH$_3$), 3.17 (s, 3H, N-CH$_3$), 3.06 (s, 3H, N-CH$_3$), 2.78–2.76 (m, 2H, C5), 2.75–2.72 (m, 2H, C6): ^{13}CNMR (CDCl$_3$) δ: 161.26, 158.36, 154.88, 153.32, 150.63, 141.27, 133.81, 129.78, 127.03, 123.14, (C-Ar), 112.73 (CN), 55.36 (O-CH$_3$), 28.71 (C5), 24.70 (C6); Anal. calc. for C$_{23}$H$_{22}$N$_4$O: C, 74.57, H, 5.99, N, 15.12. Found: C, 74.48, H, 5.95, N, 15.08.

2-amino-4-(3,4 5-trimethoxyphenyl)-9-methoxy-5,6 dihydrobenzo[f]isoquinoline-1-carbonitrile (2)

EI-MS m/z (rel. int. %): 419 (72) [M+1]$^{+}$; IR (KBr) v_{max} cm^{-1}: 3419 (NH$_2$), 2980 (C-H), 2228 (CN),1578 (C=C); ^{1}H

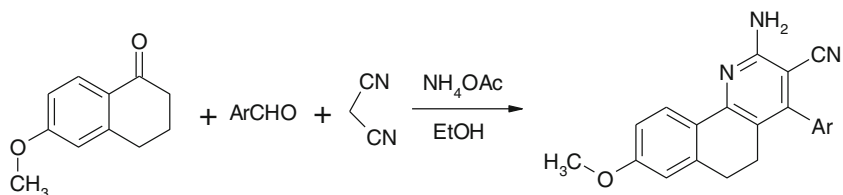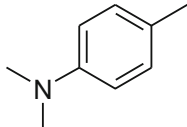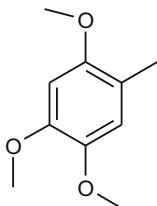**Scheme 1** Synthesis of isoquinoline derivatives
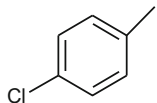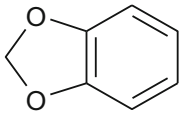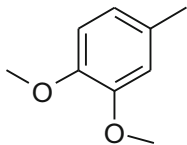
Table 1 Physicochemical data of the synthesized compounds (**1**–**5**)

Compound no.	R	Molecular formula	Crystallization	% Yield	m.p ^{o}C
1		$C_{23}H_{22}N_4O$	$CHCl_3$	78.52	181
2		$C_{24}H_{23}N_3O_4$	$CH_3OH:CHCl_3$	75.85	213
3		$C_{21}H_{16}N_3OCl$	$C_2H_5OH:CHCl_3$	73.80	201
4		$C_{22}H_{17}N_3O_3$	$CH_3OH:CHCl_3$	75.80	194
5		$C_{23}H_{21}N_3O_3$	$CHCl_3$	71.50	183

Scheme 2 Mechanism of the formation of isoquinoline derivatives
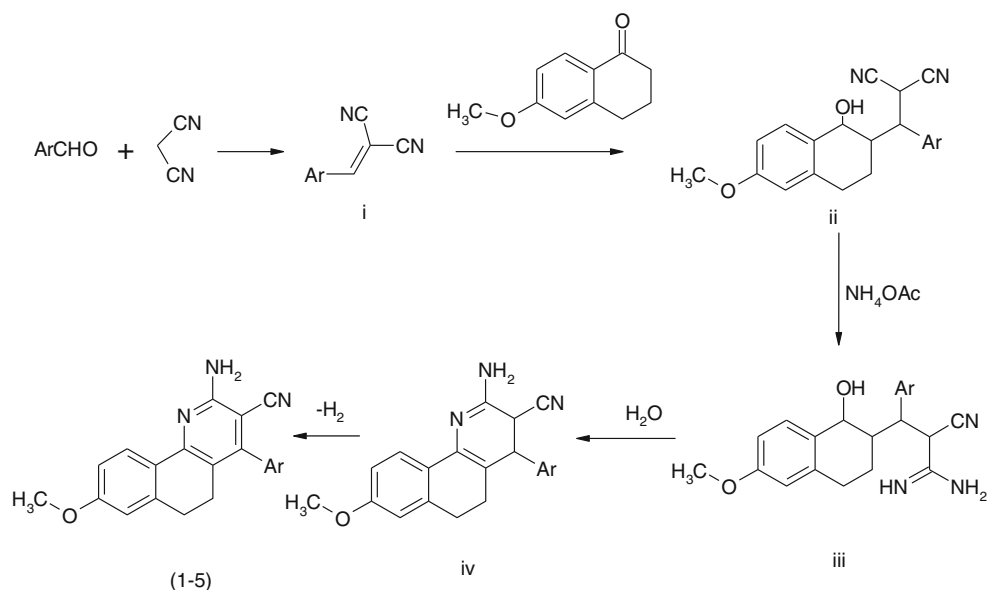
NMR (600MXz CDCl$_3$) δ:8.22 (d, 1H, CH$_{Ar}$, J=8.4 Hz), 6.89 (d, 1H, CH$_{Ar}$, J=8.4 Hz), 6.78 (d, 1H, CH$_{Ar}$, J=8.4Hz), 6.74 (s, 1H, CH$_{Ar}$), 5.07 (s, 2H, NH$_2$), 3.93 (s, 3H, OCH$_3$), 3.92 (s, OCH$_3$), 3.89 (s, 3H, OCH$_3$), 3.73 (s, 3H, OCH$_3$), 2.78–2.75 (m, 2H, C5), 2.65–2.60 (m, 2H, C6), ^{13}CNMR (CDCl$_3$) δ: 161.38, 158.04, 154.75, 154.57, 151.03, 149.90, 142.30, 145.48, 127.93, 126.78, 124.25, 122.69, 120.81 (Ar-C), 117.41(CN), 112.83, 112.73, 107.92, 90.79, 61.16, 56.04, 55.37, 28.49 (C5), 24.48 (C6); Anal. calc.for C$_{24}$H$_{23}$N$_3$O$_4$: C, 69.05, H, 5.55, N, 10.07. Found: C, 68.98, H, 5.51 N, 9.97.
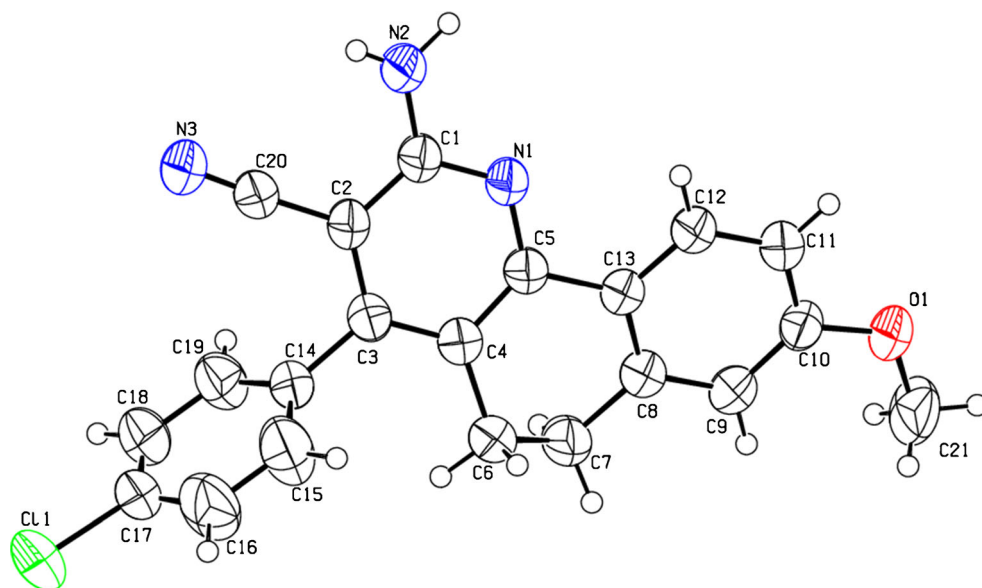
2-amino-4-(4-chlorophenyl)-9-methoxy-5,6-dihydrobenzo[f] isoquinoline-1-carbonitrile (3)

EI-MS *m/z* (rel. int. %): 363 (65) [M+1]$^+$; IR (KBr) v_{max} cm^{-1}: 3435 (NH$_2$), 2964 (C-H), 2234 (CN), 1579 (C=C); ^{1}H NMR (600MXz CDCl$_3$) δ: 8.20 (d, 1H, CH$_{Ar}$, J= 8.4 Hz), 8.02 (d, 1H, CH$_{Ar}$, J=8.4 Hz), 7.49 (d, 1H, CH$_{Ar}$, J=8.4 Hz), 7.40 (d, 1H, CH$_{Ar}$, J=8.4Hz), 6.90 (d, 1H, CH$_{Ar}$, J=3.0 Hz), 6.88 (d, 1H, CH$_{Ar}$, J=2.4 Hz), 6.72 (s, 1H, CH$_{Ar}$), 5.13 (s, 2H, NH$_2$), 3.86 (s, 3H, OCH$_3$), 2.77–2.75 (m, 2H, C5), 2.60–2.58 (m, 2H, C6); ^{13}CNMR (CDCl$_3$) δ: 161.59,

Fig. 1 Labeled *ORTEP* diagram of compound no. 3 drawn with 50 % probability level of thermal ellipsoids

158.21, 155.44, 151.48, 141.23, 134.44, 130.57, 128.10, 126.52, 119.18 (Ar-C), 117.11 (CN), 113.04, 111.87, 88.98, 55.39, 38.93, 36.07, 30.19, 28.46, 24.90 (C5), 24.57 (C6); Anal. calc.for $C_{21}H_{16}N_3OCl$: C, 69.71, H,4.46, N, 10.85. Found: C, 69.65, H, 4.42, N, 10.82.

2-amino-4-(1,3-benzodioxol-5-yl) -9-methoxy-5,6-dihydrobenzo[f]isoquinoline-1-carbonitrile (4)

EI-MS m/z (rel. int. %): 373 (65) $[M+1]^{+\cdot}$; IR (KBr) v_{max} cm^{-1}: 3432 (NH_2), 2956 (C-H), 2242 (CN), 1546 (C=C); ^1H NMR (600MXz $CDCl_3$) δ: 8.20 (d, CH_{Ar}, J=8.4 Hz), 6.89 (d, CH_{Ar}, J=3.0 Hz), 6.88 (d, CH_{Ar}, J=2.4 Hz), 6.80 (s, CH_{Ar}), 6.72 (s, CH_{Ar}), 5.10 (s, 2H, NH_2), 3.80 (s, OCH_3), 2.77–2.74 (m, 2H, C5), 2.65–2.62 (m, 2H, C6), 1.88 (s, CH_2); $^{13}CNMR$ ($CDCl_3$) δ: 161.46, 158.19, 155.21, 152.46, 148.15, 147.83, 141.27, 129.61, 128.02, 126.62, 122.42, 119.50 (Ar-C), 117.36 (CN), 112.80 (C), 109.85, 108.65, 101.47, 89.50, 77.04, 55.37, 28.54 (C5), 24.58 (C6); Anal. calc.for $C_{22}H_{17}N_3O_3$: C, 71.15, H, 4.61, N, 11.31. Found: C, 71.08, H, 4.55, N, 11.28.

Table 2 Crystal data and structure refinement for compound 3

Identification code	14,029
Empirical formula	$C_{21}H_{16}N_3OCl$
Formula weight	361.82
Temperature/K	296.15
Crystal system	triclinic
Space group	P-1
a/Å	9.2866(7)
b/Å	9.6179(10)
c/Å	11.8914(9)
α/°	101.883(7)
β/°	92.012(6)
γ/°	116.271(9)
Volume/Å^3	922.30(14)
Z	2
ρ_{calc}mg/mm^3	1.303
m/mm^{-1}	1.943
F(000)	376.0
Crystal size/mm^3	0.32×0.17×0.11
2Θ range for data collection	7.68 to 154.26°
Index ranges	−11≤h≤11, −12≤k≤11, −14≤l≤11
Reflections collected	9933
Independent reflections	3842[R(int)=0.0248]
Data/restraints/parameters	3842/0/239
Goodness-of-fit on F^2	1.055
Final R indexes [I>=2σ (I)]	R_1=0.0584, wR_2=0.1709
Final R indexes [all data]	R_1=0.0715, wR_2=0.1876
Largest diff. peak/hole / e Å^{-3}	0.59/−0.37

Table 3 Selected Bond Lengths for compound 3

Atom	Atom	Length/Å	Atom	Atom	Length/Å
Cl1	C17	1.744(2)	C6	C7	1.521(3)
O1	C10	1.370(2)	N1	C5	1.342(3)
O1	C21	1.421(3)	N2	C1	1.350(3)
N1	C1	1.338(3)	N3	C20	1.137(3)

2-amino-4-(3,4-dimethoxyphenyl) -9-methoxy-5,6-dihydrobenzo[f]isoquinoline-1-carbonitrile (5)

EI-MS m/z (rel. int. %): 390 (65) $[M+1]^{+\cdot}$; IR (KBr) v_{max} cm^{-1}: 3442 (NH_2), 2980 (C-H), 2225 (CN), 1578 (C=C); ^1H NMR (600MXz $CDCl_3$) δ: 8.20 (d, 1H, CH_{Ar}, J= 9.0 Hz), 6.99 (d, 1H, CH_{Ar}, J=8.4 Hz), 6.91 (d, 1H, CH_{Ar}, J=7.8 Hz), 6.88 (s, 1H, CH_{Ar}), 6.88 (d, 1H, CH_{Ar}, J=2.4 Hz), 6.85 (s, 1H, CH_{Ar}), 5.12 (s, 2H, NH_2), 3.94 (s, 3H, OCH_3), 3.90 (s, 3H, OCH_3), 3.85 (s, 3H, OCH_3), 2.77–2.75 (m, 2H, C5), 2.67–2.65 (m, 2H, C6); $^{13}CNMR$ ($CDCl_3$) δ: 161.44, 158.26, 155.18, 152.66, 149.51, 148.89, 141.25, 128.41, 128.00, 126.75, 121.20, 119.47 (Ar-C), 117.50 (CN), 112.79, 112.77, 111.81, 89.49, 58.50, 56.08, 55.95, 55.38, 28.60 (C5), 24.72 (C6); Anal. calc.for $C_{23}H_{21}N_3O_3$: C, 71.30, H, 5.46, N, 10.85. Found: C, 71.25, H, 5.42, N, 10.82.

Crystallography

A light yellow color single crystal with the dimension of 0.32×0.17×0.11, was taken out under microscope and fixed on sample holder consist of glass tip supported by copper pin and magnetic base. The was mounted on Agilent SuperNova (Dual source) Agilent Technologies Diffractometer, equipped withgraphite-monochromatic Cu/Mo Kα radiationfor data collectionusingCrysAlisPro software [23] at 296 K under the Cu Kα radiation. The structure solution and refinement was performed using SHELXS–97 [24], in-built with X-Seed [25]. All non–hydrogen atoms were refined anisotropically by full–matrix least squares methods [26].

All C-H atoms, which were positioned geometrically and treated as riding atoms with $C_{aromatic}$–H=0.93, $C_{methene}$–H=

Table 4 Selected bond angles for compound 3

Atom	Atom	Atom	Angle/°	Atom	Atom	Atom	Angle/°
C10	O1	C21	117.98(19)	O1	C10	C9	124.74(19)
C1	N1	C5	118.48(18)	O1	C10	C11	114.85(19)
N1	C1	N2	116.92(19)	N3	C20	C2	177.1(3)
N1	C1	C2	121.25(19)	N1	C5	C4	124.30(18)
N2	C1	C2	121.83(18)	N1	C5	C13	116.20(17)

Fig. 2 A unit cell diagram of compound no. 3 showing non classical hydrogen bonding
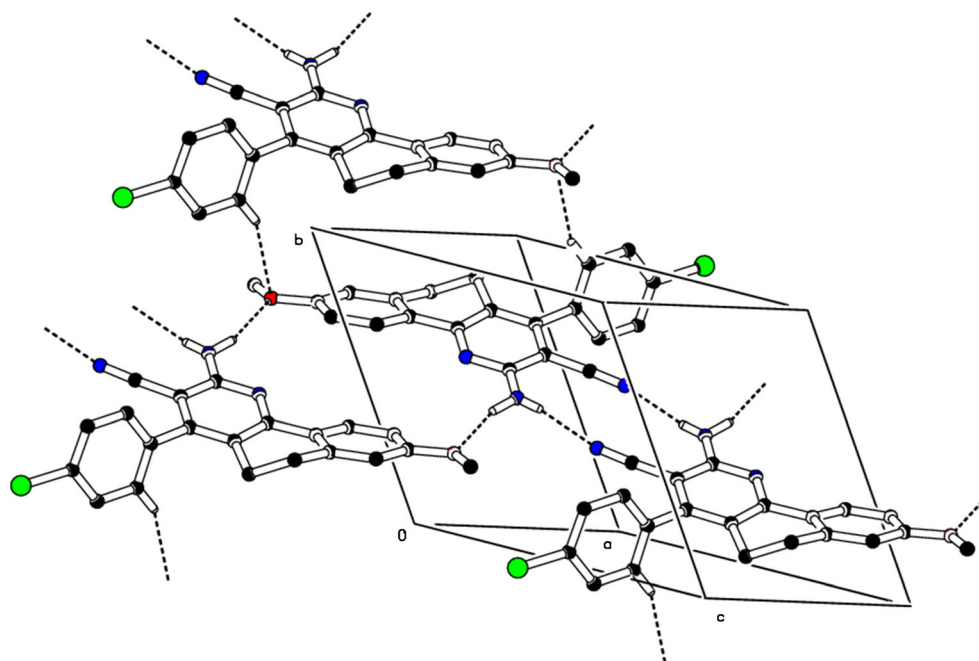
0.97, C_{methyl}–H=0.96 andUiso(H)=1.2Ueq(C) for aromatic and methylene carbon atoms while Uiso(H)=1.5Ueq(C) for methyl carbon atoms. On the other hand, the N-H=0.73(4)-0.93(2) Å, hydrogen atom were located with difference fourier map and refined using riding model with Uiso (H)=1.2 Ueq(N). CCDC 998376 contains the supplementary crystallographic data for this paper. These data can be obtained free of charge at www.ccdc.cam.ac.uk/conts/retrieving.html or from the Cambridge Crystallographic Data Centre, 12 Union Road, Cambridge CB2 1EZ, UK.

Antimicrobial Activity: Disc –Diffusion and Micro Dilution Assay

The compounds (**1**–**5**) were tested for their antibacterial activities by disc-diffusion method using nutrient broth medium [contained (g/L): beef extract 3 g; peptone 5 g; pH 7.0]. The Gram-positive bacteria and Gram-negative bacteria utilized in this study consisted of *S. aureus*, *S. pyogenes*, *S. typhimurium* and *E. coli*. The results showed that the Cyano substituted isoquinoline-1-carbonitrile increased the antibacterial activity. Among the entire five compounds, choloro substituted isoqunioline −1- carbonitrile derivative (**3**) showed better antibacterial activity than the reference drug chloramphenicol.

Computational Method

All the structures **1** to **5** studied in this paper were fully optimized by computational calculations using Density Functional Theory i.e., DFT/RB3LYP/6-31-G* level. Spartan'08 Windows graphical software is used for computation [27].

However, calculations started with Semiemperical PM3 method. Calculated geometry then submitted for the calculations with Hartree-Fock method. Finally obtained structures were calculated using Density Functional Theory with 6-31-G* basis sets.

Result and Discussion

Chemistry

Cyano substituted isoquinoline-1-carbonitrile derivatives were synthesized by one-pot multicomponent reactions (MCRs) of aldehydes, malononitrile, 6-methoxy-1,2,3,4-tetrahydro-naphthalin-1-one and ammonium acetate. However, we found that one-pot MCRs of aldehydes, malononitrile, 6-methoxy-1,2,3,4-tetrahydro-naphthalin-1-one and ammonium acetate yielded the corresponding cyano substituted isoquinoline-1-carbonitrile derivatives (Scheme 1 and Table 1). The mechanism for the formation of isoquinoline

Table 5 Hydrogen Bonds for compound 3

D	H	A	d(D–H)/Å	d(H–A)/Å	d(D–A)/Å	D–H–A/°
C15	H15	O1[1]	0.93	2.49	3.352(4)	154.3
N2	H2	O1[2]	0.93	2.28	3.172(3)	161.0
N2	H3	N3[3]	0.73(4)	2.32(4)	3.012(3)	159(4)

[1] 1-X,2-Y,-Z; [2] -X,1-Y,-Z; [3] 1-X,1-Y,1-Z

derivatives is shown in Scheme 2. The purified product was characterized by the FT-IR, ^{1}H-NMR, ^{13}C-NMR and EI MS spectra. The structures of Cyano substituted isoquinoline-1-carbonitrile derivatives were further conform by the single crustal X-ray crystallography. The formation of the Cyano substituted isoquinoline-1-carbonitrile explained according to the following mechanism (Scheme 2). The reaction seemed to be started by first addition of active hydrogen of 6-methoxy-1,2,3,4-tetrahydro-naphthalin-1-one to the ethylenic double bond of compound i. Ammonia was added to the nitrile group in ii to give iii which looses a molecule of water to give iv, which in turn was converted to the final product by auto-oxidation. The IR spectrum of compounds (1–5) shows the characteristic band at 3412–3442 cm^{-1} due to presence -NH$_2$ group and at 2218–2242 cm^{-1} attributed to the CN group. IR spectra shows sharp peek at 1234–1245 cm^{-1} due presence of C=N stretch which is conform to formation of quinoline. ^{1}H-NMR

spectra, which prove diagnostic tool for the positional elucidation of the proton. Assignments of the signals are based on chemical shift and intensity pattern. The ^{1}H-NMR spectra of all the compounds (1–5) measured at room temperature shows one singlet at 7.75–8.06 ppm for the NH$_2$. The appearance of multiplets at δ 7.29–7.62 was due to aromatic protons and two multiplets at δ 2.86–2.94 and 2.80–2.85 ppm corresponding to the benzylic protons (C5-H and C6-H respectively). Moreover, ^{13}C-NMR spectra showed signals in the range of δ 114.82–118.96 ppm and at δ 125.39–130.15 ppm due to aryl carbon and azomethine carbon, respectively. Finally characteristic peaks were observed in the mass spectra of compounds (1–5) by the molecular ion peak. The mass spectrum of compound 1 shows a molecular ion peak (M$^{+\cdot}$) m/z 372. All the compounds give similar fragmentation pattern. More evidence for the structure of compound 3 comes from its X-ray crystallography.

Fig. 3 **a** Electronic absorption spectra of 1×10^{-5} mol dm^{-3} of compound **1** in different solvents. **b** Emission spectra of 1×10^{-5} mol dm^{-3} of compound **1** in different solvents
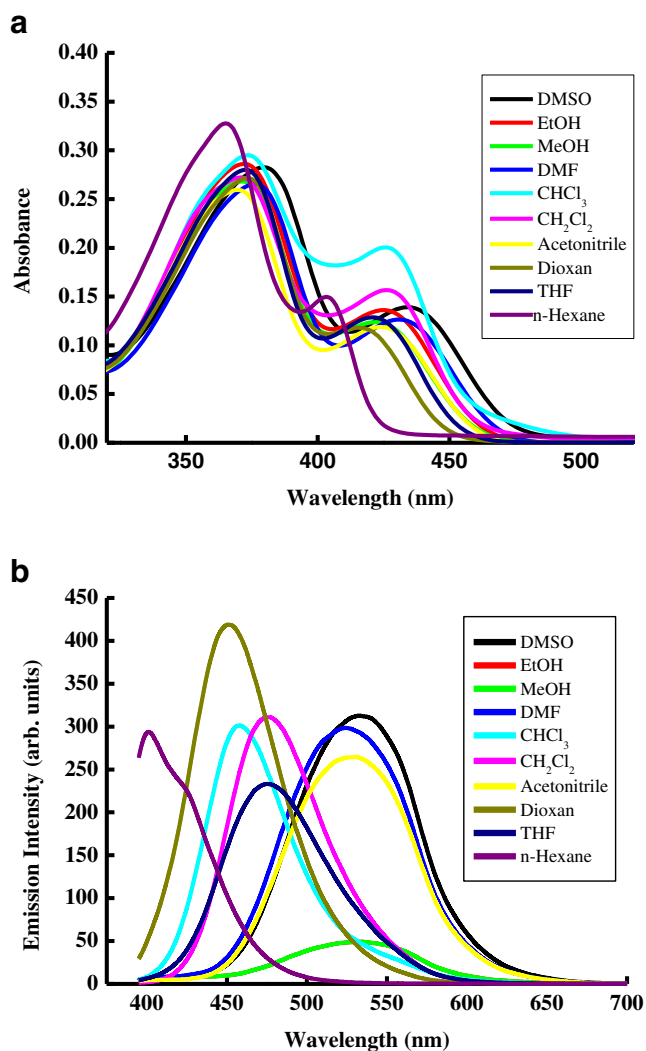
Fig. 4 **a** Electronic absorption spectra of 1×10^{-5} mol dm^{-3} of compound **2** in different solvents. **b** Emission spectra of 1×10^{-5} mol dm^{-3} of compound **2** in different solvents

X-ray Crystallography of Compound 3

In order to support the spectroscopic characteristic with the spatial arrangements of atoms in molecules we have crystalized compound 3 and diffracted at room temperature. *ORTEP* diagram shown in Fig. 1 unit cell parameters and othercrystallographic information are given in Table 2. The molecule was crystalized in triclinic crystal system with space group P −1. In molecules parent system 5,6-dihydrobenzo[*h*] quinolineconsist of an aromatic (C8-C13) **A**, pyridine (C1-C5/ N1) **B** and cyclohexadiene (C4-C8/C13) **C** rings. The puckering parameters [28] for the planes defined by atoms of cyclohexadiene are Q=0.466 (32) Å, θ=133.1(4)° and φ= 95.1(4)°. Selected bond lengths and angles are given in Tables 3 and 4 respectively. Cyclohexadiene ring is oriented at dihedral angles of 15.63 (1)° and 11.14 (1)° with pyridine and methoxy-aromatic rings respectively. 4- Chloro-phenyl ring is substituted at pyridine ring and both are twisted at

dihedral angle of 66.41 (1)°. The presence of electronegative heter-oatoms [N, O] stabilized the molecules through intermolecular interactions. NH_2 involves in two different interactions like N-H…N & N-H…O which generate twelve and twenty membered ring motifs $R_2^2(12)$ & $R_2^2(20)$ Fig. 2. On the other hand a non-classical interaction through C-H…O involves in the formation of twenty membered ring motif $R_2^2(22)$. These interactions produce an infinite one-dimensional chain along[1 0 1]base vector (Table 5).

Spectral Behavior
of 3-Cyano-2-oxo-4-substituted-1,2,5,6-tetrahydrobenzo[h] quinolines in different media

The normalized absorption spectra of cyano substituted isoquinoline dyes (**1**–**5**) in various non-polar, polar aprotic and protic solvents. Absorption and emission spectra of 1×10^{-5} mol dm^{-3} compounds (**1**–**5**) in various non-polar, polar
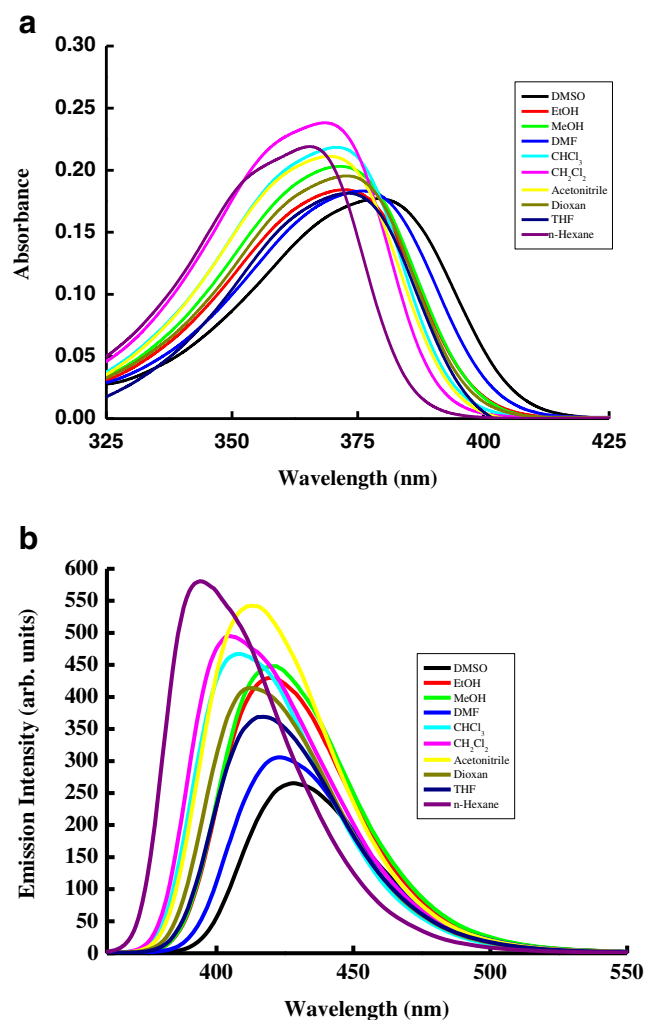
Fig. 5 a Electronic absorption spectra of 1×10^{-5} mol dm^{-3} of compound **3** in different solvents. **b** Emission spectra of 1×10^{-5} mol dm^{-3} of compound **3** in different solvents
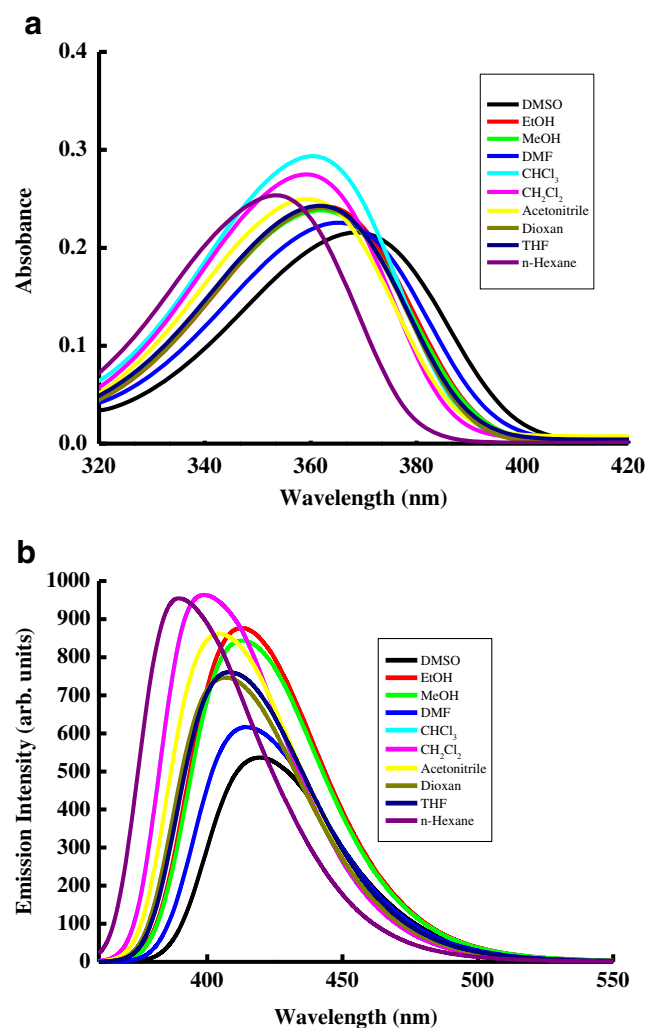
Fig. 6 a Electronic absorption spectra of 1×10^{-5} mol dm^{-3} of compound **4** in different solvents. **b** Emission spectra of 1×10^{-5} mol dm^{-3} of compound **4** in different solvents

steady state absorption and fluorescence spectra are tabulated in Tables 6, 7, 8, 9 and 10. As seen in Figs. 3a, 4, 5, 6 and 7a, polarity of solvent has a little effect on the absorption maxima. All the compounds (1–5) are red-shifts with increasing solvent polarity (dye1 shifted 17 nm, dye **2** shifted 12 nm, dye **3** shifted 15 nm, dye **4** shifted 12 and dye **5** sifted 12 nm on going from n-Hexane to DMSO) indicating some polar character of isoquinoline dues (1–5) in the ground state. These features indicate a strongly allowed π-π* transition with charge transfer characters. Compound **1** gives two absorption peaks in the range 330 to 490 with the absorption maxima at 388 to 373 (nm) and at 445–415 (nm) corresponding to transition from zero vibrational energy level in ground state to the vibrational energy level in excited state [29].

Determination of Oscillator Strength and Transition Dipole Moment

The solvatochromic behavior in compounds (**1–5**) allows one to determine the difference in the dipole moment between the excited singlet and the ground state ($\Delta\mu = \mu_e - \mu_g$). This difference can be obtained using the simplified Lippert- Mataga equation as follows [29, 30]:

$$\Delta\overline{\nu}_{st} = \frac{2\left(\mu_e - \mu_g\right)^2}{hca^3}\Delta f + Const. \tag{1}$$

$$\Delta f = \frac{D-1}{2D+1} - \frac{n^2-1}{2n^2+1} \tag{2}$$

where $\Delta\overline{\nu}_{st}$ is the Stokes–shift [31], which increases with increasing the solvent polarity pointing to stronger stabilization of the excited state in polar solvents, h denotes Planck's constant, c refers to the speed of light in vacuum and a is the

Fig. 7 **a** Electronic absorption spectra of 1×10^{-5} mol dm^{-3} of compound **5** in different solvents. **b** Emission spectra of 1×10^{-5} mol dm^{-3} of compound **5** in different solvents
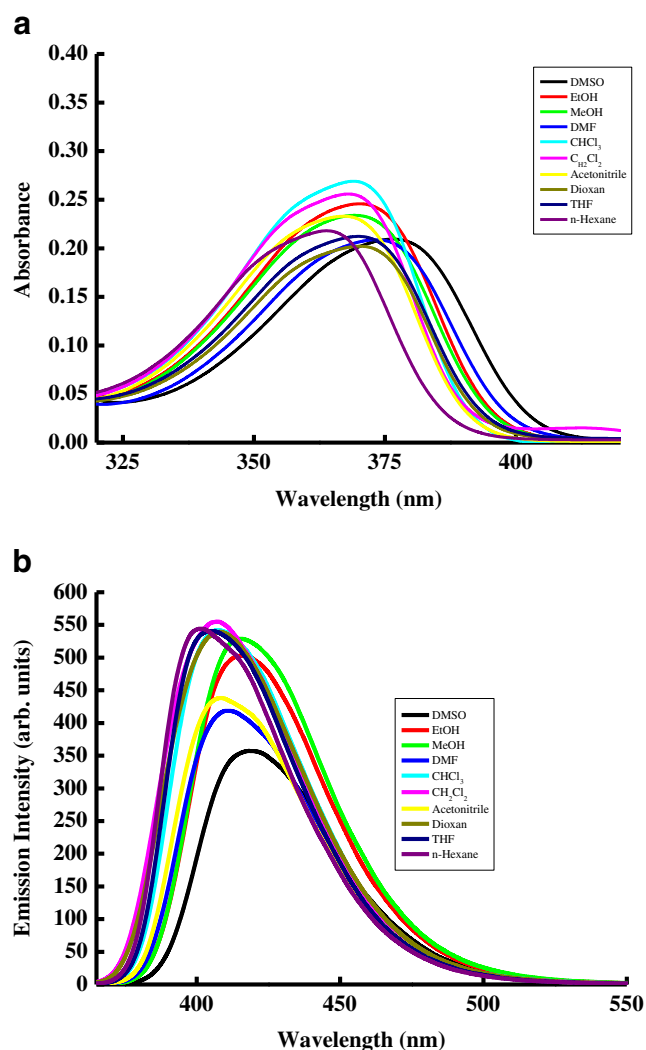
aprotic and protic solvents were studied (Figs. 3a, 4, 5, 6 and 7b). Calculated physicochemical parameters obtained from

Table 6　Spectral data and fluorescence quantum yield (φ_f) of compound no. **1** in different solvents

Solvent	Δf	E_T^N	E_T (30) Kcal mol^{-1}	λ_{ab}(nm)	λ_{em}(nm)	ε M^{-1}cm^{-1}	f	μ_{12} Debye	$\Delta\overline{\nu}$ (cm^{-1})	Φ_f
DMSO	0.266	1.31	73.31	390	530	28,310	0.76	7.68	6774	0.70
EtOH	0.305	1.37	75.23	380	527	28,288	0.88	8.36	7694	0.10
MeOH	0.308	1.37	75.23	380	535	26,760	0.81	8.06	7624	0.01
DMF	0.263	1.33	74.06	386	530	25,510	0.71	7.61	7039	0.71
CHCl$_3$	0.217	1.36	75.04	381	458	29,700	0.52	6.40	4412	0.63
CH$_2$Cl$_2$	0.255	1.36	75.23	380	475	27,310	0.57	6.70	5263	0.66
Acetonitrile	0.274	1.36	75.23	380	530	26,030	0.77	7.81	7448	0.64
Dioxan	0.148	1.35	74.65	383	475	27,160	0.45	6.00	4143	0.96
THF	0.208	1.36	75.04	381	429	28,320	0.58	6.78	5194	0.52
n-Hexane	0.0014	1.41	76.65	373	395	33,580	0.20	3.87	1493	0.52

Table 7 Spectral data and fluorescence quantum yield (φ_f) of compound no. **2** in different solvents

Solvent	Δf	E_T^N	E_T (30) Kcal mol^{-1}	λ_{ab}(nm)	λ_{em}(nm)	ε M^{-1} cm^{-1}	f	μ_{12} Debye	$\Delta\bar\nu$ (cm^{-1})	Φ_f
DMSO	0.266	1.37	75.23	380	429	22,300	0.26	4.64	3005	0.12
EtOH	0.305	1.40	76.24	375	424	25,020	0.30	4.94	3082	0.18
MeOH	0.308	1.41	76.65	373	422	24,630	0.30	4.91	3113	0.16
DMF	0.263	1.39	76.03	376	422	23,330	0.27	4.63	2899	0.13
CHCl$_3$	0.217	1.41	76.44	374	406	30,260	0.25	4.49	2107	0.15
CH$_2$Cl$_2$	0.255	1.41	76.65	373	408	28,370	0.22	4.21	2179	0.16
Acetonitrile	0.274	1.42	76.85	372	415	25,820	0.28	4.76	2785	0.16
Dioxan	0.148	1.40	76.24	375	416	24,890	0.26	4.55	2628	0.14
THF	0.208	1.40	76.24	375	419	25,070	0.28	4.71	2800	0.14
n-Hexane	0.0014	1.45	77.69	368	399	26,370	0.22	4.16	2111	0.18

Onsager cavity radius. Parameters D and n, in Eq. 2, correspond to the dielectric constant and refractive index of the solvent, respectively. The Onsager cavity radius was chosen to be 4.2 Å because this value is comparable to the radius of a typical aromatic fluorophore [32]. Stokes shifts ($\Delta\bar\nu_{ss}$) of compounds (**1–5**) in different solvents were calculated, as shown in Tables 6, 7, 8, 9 and 10, using the following the equation [29]:

$$\Delta\bar\nu_{ss} = \bar\nu_{ab} - \bar\nu_{em} \tag{3}$$

where $\bar\nu_{ab}$ and $\bar\nu_{em}$ denote the wavenumbers of absorption and emission maxima (cm^{-1}), respectively. The changes in dipole moment ($\Delta\mu$) for compounds (**1–5**) are positive value which indicates that the singlet exaited is more polar than the ground state. The values of $\Delta\mu$ are listed in Table 11.

The effective number of electrons transition from the ground to excited state is usually described by the oscillator strength, which provides the absorption area in the electronic spectrum. The oscillator strength, f, can be calculated using the following equation [33]:

$$f = 4.32 \times 10^{-9} \int \varepsilon\left(\bar\nu\right) d\bar\nu \tag{4}$$

where ε is the extinction coefficient (Lmol^{-1} cm^{-1}), and $\bar\nu$ represents the numerical value of wavenumber (cm^{-1}). Oscillator strength values of compounds (**1–5**) in different solvents are reported in Tables 6, 7, 8, 9 and 10. In addition, the transition dipole moment (μ) for compounds (**1–5**) from ground to excited state in Debye was estimated in different solvents (Table 11) using the following relation [34]:

$$\mu^2 = \frac{f}{4.72 \times 10^{-7} \times E_{max}} \tag{5}$$

where E_{max} is the maximum energy of absorption in cm^{-1}

Table 8 Spectral data and fluorescence quantum yield (φ_f) of compound no. **3** in different solvents

Solvent	Δf	E_T^N	E_T (30) Kcal mol^{-1}	λ_{ab}(nm)	λ_{em}(nm)	ε M^{-1} cm^{-1}	f	μ_{12} Debye	$\Delta\bar\nu$ (cm^{-1})	Φ_f
DMSO	0.266	1.35	74.65	383	430	17,800	0.20	4.05	2854	0.16
EtOH	0.305	1.39	75.83	377	425	18,400	0.22	4.19	2996	0.25
MeOH	0.308	1.39	76.03	376	425	20,300	0.24	4.44	3066	0.23
DMF	0.263	1.36	75.04	381	427	18,360	0.20	4.08	2827	0.18
CHCl$_3$	0.217	1.39	76.03	376	412	21,900	0.20	4.02	2324	0.23
CH$_2$Cl$_2$	0.255	1.40	76.24	375	410	22,700	0.20	4.05	2276	0.23
Acetonitrile	0.274	1.41	76.44	374	418	21,200	0.23	4.34	2814	0.27
Dioxan	0.148	1.38	75.63	378	416	19,580	0.18	4.89	2417	0.23
THF	0.208	1.38	75.63	378	421	18,210	0.19	4.96	2703	0.22
n-Hexane	0.0014	1.43	77.27	370	398	22,140	0.16	4.62	1902	0.28

Table 9 Spectral data and fluorescence quantum yield (φ_f) of compound no. **4** in different solvents

Solvent	Δf	E_T^N	E_T (30) Kcal mol^{-1}	λ_{ab}(nm)	λ_{em}(nm)	ε M^{-1} cm^{-1}	f	μ_{12} Debye	$\Delta\bar{\nu}$ (cm^{-1})	Φ_f
DMSO	0.266	1.36	74.84	382	427	20,340	0.25	4.56	3176	0.22
EtOH	0.305	1.39	76.03	376	420	25,930	0.28	4.79	2786	0.25
MeOH	0.308	1.40	76.24	375	419	22,000	0.24	4.36	2800	0.23
DMF	0.263	1.38	75.43	379	421	23,690	0.24	4.38	2633	0.19
CHCl$_3$	0.217	1.41	76.44	374	409	31,400	0.28	4.76	2288	0.26
CH$_2$Cl$_2$	0.255	1.41	76.44	374	406	23,330	0.19	3.94	2107	0.25
Acetonitrile	0.274	1.41	76.65	373	413	25,430	0.26	4.56	2596	0.16
Dioxan	0.148	1.39	76.03	376	413	22,510	0.21	4.12	2382	0.21
THF	0.208	1.39	75.83	377	417	22,470	0.22	4.19	2545	0.18
n-Hexane	0.0014	1.44	77.48	369	393	23,990	0.15	3.42	1655	0.25

Fluorescence Polarity Study of Compounds (1–5)

The emission spectra of the 1×10^{-5} M of dyes (**1–5**) were measured in various polar aportic and polar protic solvents and shown in Figs. 3b, 4, 5, 6 and 7b. Their spectral data are also collected in Tables 6, 7, 8, 9 and 10. The emission spectra of these **dyes** (**1–5**) consist of one broad band in different solvents. This band can be assigned to S_1-S_0 electronic transition. All the compounds gives the same behavior i.e., dyes show red shift with increasing solvent polarity (n-Heptane to DMSO). Dye **1** shifted 135 nm dye **2** shifted 30 dye **3** shifted 32 dye **4** shifted 34 and dye **5** shifted 19 nm on going from n-Heptane to DMSO indicating the involvement of photoinduced intramolecular charge transfer (ICT) in the singlet excited state than in ground state. The solvent dependence of fluorescence spectra has some time called solvatoflurchromism. We found that the dye **1** shoed the interesting solvatofluorchromic property in various solvents. The emission maximum of dye **1** is bathchromic shifted 135 nm from 395 to 530 nm changing the solvent from n-Hexane to DMSO.

The empirical Dimroth polarity parameter, E_T (30) and E_T^N of dyes (**1–5**) was also calculated according to the following equation [35, 36].

$$E_T^N = \frac{E_T(solvent) - 30.7}{32.4} \tag{6}$$

$$E_T(solvent) = \frac{28591}{\lambda_{max}} \tag{7}$$

where λ_{max} corresponds to the peak wavelength (nm) in the red region of the intramolecular charge transfer absorption of all compounds. The red (bathochromic) shift from n-hexane to DMSO indicates that photoinduced intramolecular charge transfer (ICT) occurs in the singlet excited state, and the polarity of compounds, therefore, increases on excitation.

The fluorescence quantum yield (φ_f) was measured using the optically diluted solution to avoid reabsorption effect

Table 10 Spectral data and fluorescence quantum yield (φ_f) of compound no. **5** in different solvents

Solvent	Δf	E_T^N	E_T (30) Kcal mol^{-1}	λ_{ab}(nm)	λ_{em}(nm)	ε M^{-1} cm^{-1}	f	μ_{12} Debye	$\Delta\bar{\nu}$ (cm^{-1})	Φ_f
DMSO	0.266	1.36	75.04	381	424	21,030	0.22	4.21	2662	0.30
EtOH	0.305	1.39	76.03	376	420	24,600	0.27	4.63	2786	0.23
MeOH	0.308	1.40	76.24	375	419	23,400	0.26	4.54	2800	0.25
DMF	0.263	1.38	75.63	378	415	21,010	0.19	3.90	2359	0.19
CHCl$_3$	0.217	1.40	76.24	375	413	26,980	0.26	4.54	2453	0.22
CH$_2$Cl$_2$	0.255	1.41	76.44	374	413	25,600	0.25	4.45	2524	0.24
Acetonitrile	0.274	1.42	76.85	372	412	23,400	0.24	4.34	2610	0.26
Dioxan	0.148	1.39	76.03	376	411	20,310	0.18	4.78	2265	0.21
THF	0.208	1.39	76.03	376	410	21,290	0.18	4.78	2205	0.22
n-Hexane	0.0014	1.44	77.48	369	405	21,970	0.21	4.05	2409	0.28

Table 11 Change in Δμ of compounds (**1–5**)

Compound	Δμ (Debye)
1	12.31
2	4.54
3	5.02
4	5.13
5	3.09

Table 13 Minimum inhibition concentration (MIC) of isoquinoline derivatives (**1–5**)

Bacterial strain	MIC (μg mL^{-1} compound)					Positive control
	1	2	3	4	5	
S. aureus	128	128	32	128	256	32
S. pyogenes	64	64	16	256	128	32
S. typhimurium	256	64	32	128	128	32
E. coli	128	128	32	128	64	32

Positive control: chloramphenicol (Chlora.) Negative control: (DMSO)

(absorbance at excition wave relative method with solution of 9, 10-diphenylanthralene (DPA) in DMSO as reference standard [37, 38]. The following relation has applied to calculate the fluorescence quantum yield:

$$\phi_f(s) = \varphi_f(r) \frac{F_{(s)} \left\{ 1-\exp\left(-A_{ref}\ \ln 10\right) \right\} \times n^2 s}{F_{(ref)} \left\{ 1-\exp\left(-A_s \ln 10\right) \right\} \times n^2 r} \tag{8}$$

Where F denotes the integral of the corrected fluorescence spectrum, A is the absorbance at the excitation wavelength, and n is the refractive index of the medium. The subscripts "s" and "r" refer to sample and reference, respectively. Flurescence quantum yield of dyes (**1–5**) in different solvent are also listed Tables 6, 7, 8, 9 and 10.

In Vitro Screening: Disc –Diffusion and Micro Dilution Assay

Antibacterial activity was done by the disk diffusion method with minor modifications. *S. aureus*, *S. pyogenes*, *S. typhimurium* and *E. coli* were sub-cultured in BHI medium and incubated for 18 h at 37 °C, and then the bacterial cells were suspended, according to the McFarland protocol in saline solution to produce a suspension of about 10^{-5} CFU mL^{-1}: 10 μL of this suspension was mixed with 10 mL of sterile nutrient agar at 40 °C and poured onto an agar plate in a laminar flow cabinet [39, 40]. Five paper disks (6.0 mm diameter) were fixed onto nutrient agar plate. One milligram of each test compound was dissolved in 100 μl DMSO to

prepare stock solution from stock solution different concentration 10, 20, 25, 50, and 100 μg/ μl of each test compound were prepared. These compounds of different concentration were poured over disk plate on to it. Chloramphenicol (30 μg/ disk) was used as standard drug (positive control). DMSO poured disk was used as negative control. The susceptibility of the bacteria to the test compounds was determined by the formation of an inhibitory zone after 18 h of incubation at 36 °C (Table 12) reports the inhibition zones (mm) of each compound and the controls. The minimum inhibitory concentration (MIC) was evaluated by the macro dilution test using standard inoculums of 10^{-5} CFL mL^{-1}. Serial dilutions of the test compounds, previously dissolved in dimethyl sulfoxide (DMSO) were prepared to final concentrations of 512, 256, 128, 64, 32, 16, 8, 4, 2 and 1 μg/ mL to each tube was added 100 μL of a 24 h old inoculum. The MIC, defined as the lowest concentration of the test compound, which inhibits the visible growth after 18 h, was determined visually after incubation for 18 h, at 37 °C, and the results are presented in Table 13. Tests using DMSO and chloramphenicol as negative and positive controls.

Cytotoxicity Against L123 (Human Lung Cells)

Cytotoxicity was performed by MTT assay method [41]. A 96 well flat bottom tissue culture plate was seeded with 2×10^3

Table 12 Antibacterial activity and cytotoxicity profile of compounds **1–5**

Compounds	Zone of inhibition ZOI (mm)				Cytotoxicity IC$_{50}$ (mM/mL)
	S. aureus	*S.Pyogenes*	*S.typhimurium*	*E. coli*	
1	13.6±0.4	12.7±0.4	13.4±0.5	14.5±0.5	>200
2	14.4±0.3	14.5±0.3	11.4±0.2	11.2±0.2	>100
3	21.2±0.3	22.4±0.4	19.6±0.4	23.2±0.4	50
4	12.3±0.3	14.2±0.5	11.3±0.4	12.4±0.3	>100
5	13.0±0.4	13.8±0.3	11.5±0.4	11.8±0.5	50
Chlora.	17.0±0.5	18.2±0.4	17.2±0.8	20.0±0.2	
DMSO	–	–	–	–	

Positive control: chloramphenicol (Chlora.); Negative control: (DMSO) measured by the Halo Zone Test (Unit, mm)

Table 14 Total energy, E_{HOMO}, E_{LUMO}, Energy gap (Eg) and dipole moment calculated using B3LYP/6-31+G* level of theory

Compound	Total energy (au)	Dipole moment (debye)	E_{HOMO} (eV)	E_{LUMO} (eV)	Eg (eV)
1	−1104.14945	2.54	−5.91	−1.95	3.96
2	−2.04	3.94	−5.85	−1.91	3.94
3	−1508.38531	5.28	−6.06	−2.14	3.92
4	−1237.32641	3.93	−5.98		
5	−1277.83592	2.76	−5.95	−2.01	3.94

cells in 0.1 mL of MEM medium supplemented with 10 % FBS and allowed to attach for 24 h. After 24 h of incubation, cells were treated with test compounds to get a concentration of 5, 10, 20, 50 and 100 mM/mL incubated for 48 h. The cells in the control group received only the medium containing the 0.2 % DMSO. Each treatment was performed in duplication. After the treatment, drug containing media was removed and washed with 200 mL of PBS. To each well of the 96 well plate, 100 mL of MTT reagent (stock: 1 mg/mL in serum free medium) was added and incubated for 4 h at 37 °C. After 4 h of incubation the plate was inverted on tissue paper to remove the MTT reagent. To solubilize formazan crystals in the wells, 100 mL of 100 % DMSO was added to each well. The optical

density was measured by microtiter plate reader at 590 nm. Compound concentration (mM) required to reduce the viability of mockinfected cells by 50 % as determined by MTT method which summarized in Table 12. Results of MTT assay mentioned on the cell viability based on ability to metabolize the compounds. The results show that compound **1** is comparatively more cytotoxic than **2** and **4**, compound no **3** is the less cytotoxic as these derivatives showed IC50 values more than 100 mM/mL.

Computation

All the structures **1** to **5** studied in this paper were investigated by computational calculations using DFT/RB3LYP/6-31-G* level of theory. Some selected descriptors such as total energy, dipole moment, LUMO (Lowest Unoccupied Molecular Orbital), HOMO (Highest Occupied Molecular Orbital) and energy gap (Eg) i.e., the energy difference between LUMO and HOMO, are summarized in Table 14. All the 3D optimized structure in this studied are shown in Fig. 8

In this study the structure **3** that is chloro benzene substituted isoqunioline-1-carbonitrile seemed to confer higher antibacterial potency than that of all the other studied compounds. This compound is characterized by lowest LUMO energy value as compared to all other studied compounds. The Frontier

Fig. 8 Fully optimized structures **1** to **5** calculated with DFT/RB3LYP method
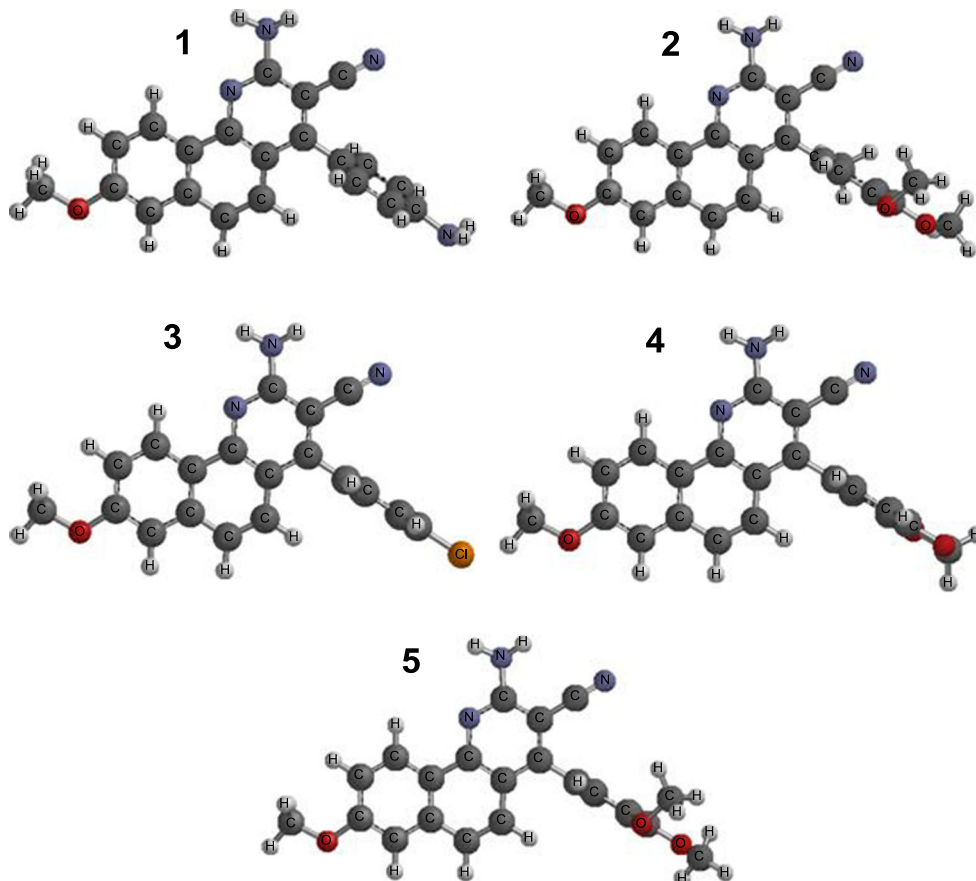
Molecular Orbital is crucial in predicting the reactivity of a species. Antibacterial activity of a molecule is a function of its molecular orbitals (LUMO and HOMO). Molecules with low-lying LUMO are more capable to accept electrons than those with higher energy LUMO and thus will show higher activity.

It was observed that the molecule **3** has the lowest LUMO energies values (-6.06 eV). Thus, one can conclude the higher antibacterial activity of compounds **3**. However the energy gap of this compound is also found lowest than the others, this result also supports its higher activities. The HOMO and the LUMO maps were generated for compounds **1** to **5** and are given in Fig. 9. The graph of molecular orbitals of the compounds infers that electron density is more localized on benzoquinoline structure. However, when compared the LUMOs of all the structures, it was found that compound **3** has comparatively large LUMO at the Chloro-benzene structure attached to the bezoquinoline, which is comparatively less or not present in all other structures (**1**, **2**, **4**, **5**). However, when come to dipole moment compound **3** has also shown the highest dipole moment that is 5.28 debye, this property also designates its highest activity.

These results indicate that the possible role of the benzoquinoline and its attached chloro-benzene group (compound **3**) is the charge transfer processes in ligand-protein target interaction. These theoretical results are in good agreement in our experimental results. Antibacterial activity is probably affected by these electronic descriptors, which can be important parameters for the interaction of the studied compounds with the active sites.

Fig. 9 The schematic representation of HOMO and LUMO density map of all the compounds **1**–**5** is shown
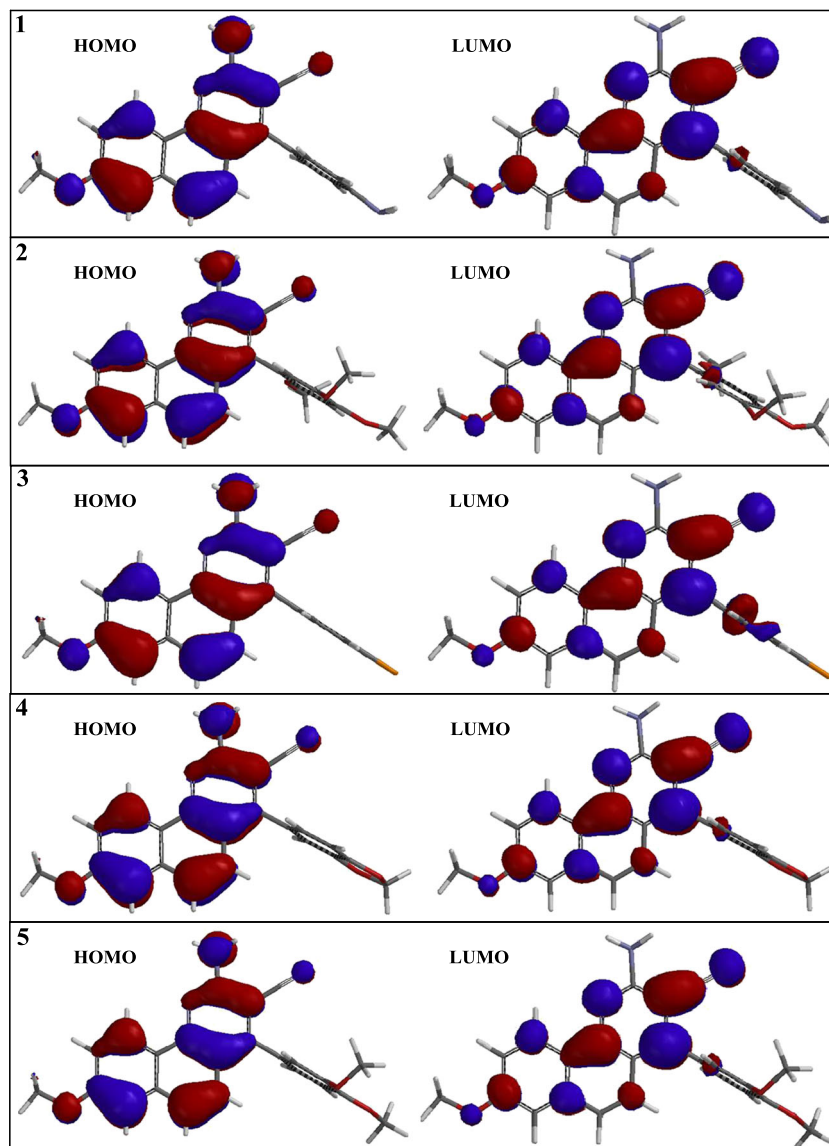
Conclusion

Cyano substituted isoquinoline-1-carbonitrile derivative were synthesized by one-pot multicomponent reactions (MCRs) of aldehydes, malononitrile, 6-methoxy-1,2,3,4-tetrahydro-naphthalin-1-one and ammonium acetate. In addition, studying spectroscopic and physicochemical properties of Cyano substituted isoquinoline-1-carbonitrile derivatives may show considerable promise towards their potential applications. The antibacterial activity of these compounds was investigated using culture of bacteria. Results demonstrated that the Cyano substituted isoquinoline-1-carbonitrile derivative increased the antibacterial activity. Among the entire five compounds, choloro substitutrd isoqunioline −1- carbonitrile derivative (**3**) showed better antibacterial activity than the reference drug chloramphenicol. Indeed, our theoretical results corroborate to the experimental results as well. Physicochemical studies of the compounds including singlet absorption, extinction co-efficient, Stokes shift, oscillator strength, dipole moment and fluorescence quantum yield were investigated on the basis of the polarity of solvent.

References

1. Chinnaraja D, Rajalakshmi R, Srinivasan T, Velmurugan D, Jayabharathi J (2014) Spectral studies of 2- pyrazoline derivatives: structural elucidation through single crystal XRD and DFT calculations. Spectrochim Acta A 124:3033

2. Wang N, Switalska M, Wu M, Imai K, Ngoc TA, Pang C, Wang L, Wietrzyk J, Inokuchi T (2014) Synthesis and in vitro cytotoxic effect of 6-amino-substituted 11*H*- and 11Me-indolo[3,2-*c*] quinolines. Eur J Med Chem 78:314–323

3. Kumar KK, Seenivasan SP, Kumar V, Das TM (2011) Synthesis of quinoline coupled [1,2,3]-triazoles as a promising class of anti-tuberculosis agents. Carbohydr Res 346:2084–2090

4. Tabatabaeian K, Shojaei AF, Shirini F, Hejazi SZ, Rassa M (2014) A green multicomponent synthesis of bioactive pyrimido[4,5-b] quinoline derivatives as antibacterial agents in water catalyzed by RuCl$_3$·xH$_2$O. Chin Chem Lett 25:308–312

5. Hayat F, Salahuddin A, Umar S, Azam A (2010) Synthesis, characterization antiamoebic activity and cytotoxicity of novel series of pyrazoline derivatives bearing quinoline tail. Eur J Med Chem 45: 4669–4675

6. Gopal M, Shenoy S, Doddamani LS (2003) Antitumor activity of 4-amino and 8-methyl-4-(3diethylamino propylamino)pyrimido[4′,5′: 4,5]thieno (2,3-*b*) quinolines. J Photochem Photobiol B 72:1–3

7. Bedoya LM, Abadn MJ, Calonge E, Saavedra LA, Gutierrez M, Kouznetsov VV, Alcami J, Bermejo P (2010) Quinoline-based compounds as modulators of HIV transcription through NF-κB and Sp1 inhibition. Antiviral Res 87:338–344

8. Kato J, Ijuin R, Aoyama H, Yokomatsu T (2014) Synthesis of poly-substituted pyrazolo[1,5-*a*]quinolines through one-pot two component cascade reaction. Tetrahedron 70:2766–2775

9. Gonzalez-Sanchez I, Solano JD, Loza-Mejia MA, Olvera-Vazquez S, Rodriguez-Sotres R, Morán J, Lira-Rocha A, Cerbon MA (2011) Antineoplastic activity of the thiazolo [5,4-b] quinoline derivative D3CLP in K-562 cells is mediated through effector caspases activation. Eur J Med Chem 46:2102–2108

10. Jha RR, Aggarwal T, Verma AK (2014) Stereoselective tandem synthesis of oxazolo-fused pyrroloquinolines from *o*-alkynylaldehydes via Ag(I)-catalyzed regioselective 5-*exo-dig* ring closure. Tetrahedron Lett 55:2603–2608

11. Zhang J, Pan M, Yang R, She Z, Kaim W, Fan Z, Su C (2010) Structure, biological and electrochemical studies of transition metal complexes from N, S, N′ donor ligand 8-(2-pyridinylmethylthio)quinoline. Polyhedron 29:581–591

12. Bala BD, Muthusaravanan S, Perumal S (2013) An expedient synthesis of 1,2-dihydrobenzo[*g*]quinoline-5,10-diones via copper(II) triflate-catalyzed intramolecular cyclization of *N*-propargylaminonaphthoquinones. Tetrahedron Lett 54:3735–3739

13. Paredes E, Biolatto B, Kneetmann M, Mancini P (2002) One-step synthesis of 2,9-disubstituted phenanthrenes via Diels–Alder reactions using 1, disubstituted naphthalenes as dienophiles. Tetrahedron Lett 43:4601–4603

14. Kachkovsky AD, Pilipchuk NV, Kurdyukov VV, Tolmachev AI (2006) Electronic properties of polymethine systems. 10. Electron structure and absorption spectra of cyanine bases. Dyes Pigments 70:212–219

15. Zhu S, Lin W, Yuan L (2013) Development of a ratiometric fluorescent pH probe for cell imaging based on a coumarin–quinoline platform. Dyes Pigments 99:465–471

16. Zhou B, Liang L, Yao J (2014) Effects of isomorphous substitution of a coordination polymer on the properties and its application inelectrochemical sensing. J Solid State Chem 215:109–113

17. Pyszka I, Kucybała Z (2007) Quinolineimidazopyridinium derivatives as visible-light photoinitiators of free radical polymerization. Polymer 48:959–965

18. El-Daly SA, Asiri AM, Obeid AY, Khan SA, Alamry KA, Hussien MH, Al-Sehemi AG (2013) Photophysical parameters and laser activity of 3(4-dimethylamino-phenyl)-1-(2, 5-dimethyl-thiophen-3-yl)-propenone (DDTP): a new potential laser dye. Opt Laser Technol 45:605–612

19. Mansour AM, Hassaneen HM, Mohammed YS, Ghani NTA (2013) Single crystal, spectral, computational studies and in vitro cytotoxicity of 2-chloro-3-formylpyrido[2-,1-a]isoqoinoline −1-carbonitrile derivative. J Mol Struct 1045:180–190

20. Raman N, Selvaganapathy M (2013) Pyrazolone incorporating amino acid metallointercalators as effective DNA targets: synthesis and in vitrobiocidal evaluation. Inorg Chem Commun 37:114–120

21. Arion VB, Jakupec MA, Galanski M, Unfried P, Keppler BK (2002) Synthesis, structure, spectroscopic and in vitro antitumour studies of a novel gallium(III) complex with 2-acetylpyridine ^4N-dimethylthiosemicarbazone. J Inorg Biochem 91:298–305

22. Aly SA, El-Ezabawy SR, Abdel-Fattah AM (1991) Reactions with α-substituted cinnamonitriles: synthesis of benzo[h]quinolines and naphtho[1,2, b] pyrans. Egypt J Pharm Sci 32:827–834

23. PRO Agilent CrysAlis (2012) Agilent technologies. Yarnton, England

24. Sheldrick GM (2008) A short history of SHELX. Acta Crystallogr A64:112–122

25. Barbour LJ, Seed X (2001) A software tool for supramolecular crystallography. J Supramol Chem 1:189

26. Bernstein J, Davis RE, Shimoni L, Chang NL (1995) Patterns in hydrogen bonding functionality and graph set analysis in crystals. Angew Chem Int Ed Engl 34:1555–1573

27. Spartan'08 Version 1.2.0, Wavefunction, Inc., 18401 Von Karman Ave., Suite 370, Irvine, CA 92612, USA

28. Cremer D, Pople JA (1975) General definition of ring puckering coordinates. J Am Chem Soc 97:1354–1358

29. Lippert E (1957) Spectroscopic determinations of the dipole moment of aromatic compounds in the first excited singlet state. Z Electrochem 61:962–975

30. Marwani HM, Asiri AM, Khan SA (2013) Spectral, stoichiometric ratio, physicochemical, polarity and photostability studies of newly synthesized chalcone dye in organized media. J Lumin 136: 296–302

31. Asiri AM, El-Daly SA, Khan SA (2012) Spectral characteristics of 4-(p-N, N-dimethyl-aminophenylmethylene)-2-phenyl-5-oxazolone (DPO) in different media. Spectrochimica Acta A 95:679–684

32. Kumarn S, Rao VC, Rastogi RC (2001) Excited-state dipole moments of some hydroxycoumarin dyes using an efficient solvatochromic method based on the solvent polarity parameter. ETN Spectrochim Acta A 57:41–47

33. El-Daly SA, Asiri AM, Khan SA, Alamry KA, Hussein MA (2011) Chin J Chem 29:2557–2561

34. Asiri AM, Marwani HM, Alamry KA, Al-Amoudi MS, Khan SA, El-Daly SA (2014) Green synthesis, characterization, photophysical and electrochemical properties of Bis-chalcones. Int J Electrochem Sci 9: 799–809

35. Turro NJ (1965) Molecular photochemistry (frontiers in chemestry), 1st edn. W. A. Benjamin, Inc., Reading, p 286

36. El-Daly SA, Asiri AM, Alamry KA, Khan SA (2013) Spectroscopic studies and laser activity of 3-(4-Dimethylamino-phenyl)-1-(2, 5-dimethyl-furan-3-yl)- propenone (DDFP): a new green laser dye. J Lumine 137:6–14

37. El-Daly SA, Asiri AM, Khan SA, Alamry KA (2013) Spectral properties and Micellization of 1-(2, 5-Dimethyl-thiophen-3-yl)-3-(2,4-5-trimethoxy-phenyl)-propenone (DTTP) in Fifferent media. J Lumine 134:819–824

38. Asiri AM, Marwani HM, Khan SA, El-Daly SA (2013) Investigation of spectroscopic behaviors of newly synthesized (2E) -3-(3,4-dimethoxyphenyl)-1-(2,5-dimethylthiophen-3-yl)prop-2-en-1one(DDTP)dye. J Fluresc 23:1271–1278

39. Khan SA, Asiri AM (2012) Synthesis and in vitro antibacterial activity of novel steroidal (6R)-Spiro-1,3,4-thiadiazoline derivatives. J Heterocycl Chem 49:1452–1457

40. Asiri AM, Khan SA, Marwani HM, Sharma K (2013) Synthesis, spectroscopic and physicochemical investigations of environmentally benign heterocyclic Schiff base derivatives as antibacterial agents on the bases of in vitro and density functional theory. J Photochem Photobiol B 120:82–89

41. Piotrowska DG, Cieślak M, Krolewska K, Wroblewskin AE (2011) Design, synthesis and cytotoxicity of a new series of isoxazolidines derived from substituted chalcones. Eur J Med Chem 46:1382–1389